

| REPORT DOCUMENTATION PAGE | | READ INSTRUCTIONS BEFORE COMPLETING FORM |
|--|-----------------------|---|
| 1. REPORT NUMBER ARCCB-TR-89002 | 2. GOVT ACCESSION NO. | 3. RECIPIENT'S CATALOG NUMBER |
| 4. TITLE (and Subtitle) STRESS CORROSION CRACKING OF A723 STEEL PRESSURE VESSELS: TWO CASE STUDIES | | 5. TYPE OF REPORT & PERIOD COVERED Final |
| | | 6. PERFORMING ORG. REPORT NUMBER |
| 7. AUTHOR(s) J. H. Underwood and J. J. Miller (See Reverse) | | 8. CONTRACT OR GRANT NUMBER(s) |
| 9. PERFORMING ORGANIZATION NAME AND ADDRESS US Army ARDEC Benet Laboratories, SMCAR-CCB-TL Watervliet, NY 12189-4050 | | 10. PROGRAM ELEMENT, PROJECT, TASK AREA & WORK UNIT NUMBERS AMCMS No. 694000084 PRON No. AW6MC00103AW1A |
| 11. CONTROLLING OFFICE NAME AND ADDRESS US Army ARDEC Close Combat Armaments Center Picatinny Arsenal, NJ 07806-5000 | | 12. REPORT DATE January 1988 |
| | | 13. NUMBER OF PAGES 33 |
| 14. MONITORING AGENCY NAME & ADDRESS (if different from Controlling Office) | | 15. SECURITY CLASS. (of this report) UNCLASSIFIED |
| | | 15a. DECLASSIFICATION/DOWNGRADING SCHEDULE |
| 16. DISTRIBUTION STATEMENT (of this Report) Approved for public release; distribution unlimited. | | |
| 17. DISTRIBUTION STATEMENT (of the abstract entered in Block 20, if different from Report) | | |
| 18. SUPPLEMENTARY NOTES Presented at the ASME 1986 Pressure Vessel and Piping Conference, Chicago, IL, 21-25 July 1986. Published in Proceedings of the Conference. | | |
| 19. KEY WORDS (Continue on reverse side if necessary and identify by block number) Stress Corrosion Fracture Mechanics Pressure Vessels High Strength Steel Residual Stress Fatigue Cannon | | |
| 20. ABSTRACT (Continue on reverse side if necessary and identify by block number) Two separate investigations of apparent stress corrosion cracking of cannon tubes under field service conditions are described. The first investigation involved several tubes in which cracking initiated at the inner diameter surface due to the combination of cannon firing products and tensile residual stresses. Results of metallographic and fracture surface studies; residual stress measurements; fatigue life and material mechanical tests; and stress corrosion simulation tests of tube sections are presented and discussed. (CONT'D ON REVERSE) | | |

7. AUTHORS (CONT'D)

J. J. Miller
Product Assurance Directorate
Watervliet Arsenal
Watervliet, NY 12189-4050

20. ABSTRACT (CONT'D)

The second investigation involved two tubes in which apparent stress corrosion cracking occurred on the outer diameter surface due to the combination of an unknown substance, presumed to be a cleaning product, and tensile residual stress due to autofrettage of the tube.

The critical requirements for stress corrosion cracking are discussed in general and in relation to the pressure vessels of the two investigations. Conclusions are drawn regarding design and service conditions for pressure vessels which will help prevent the occurrence of stress corrosion cracking. *Keywords:*

FATIGUE (mechanics), Fatigue Life,
Fatigue Tests (mechanics) • (-

UNCLASSIFIED

DEDICATION

This report is dedicated to the late Joseph R. Pape, Product Assurance Directorate, Watervliet Arsenal. Mr. Pape applied his outstanding combination of enthusiasm, cooperativeness, and technical competence to the work described here.



| | |
|--------------------|--|
| Accession For | |
| NTIS GRA&I | <input checked="checked" type="checkbox"/> |
| DTIC TAB | <input type="checkbox"/> |
| Unannounced | <input type="checkbox"/> |
| Justification | |
| By | |
| Distribution/ | |
| Availability Codes | |
| Dist | Avail and/or Special |
| A-1 | |

ACKNOWLEDGEMENTS

We are pleased to credit Mr. B. Brown and co-workers for design and execution of tube fatigue tests; Mr. L. McNamara and Mr. C. Rickard for fractographic and metallographic analyses; Mr. G. Capsimalis and co-workers for x-ray residual stress measurements; Dr. J. Kapp and Mr. F. Moscinski for environmental testing; and Mr. R. McNeill and E. Fogarty for manuscript preparation.

We are also pleased to acknowledge the help of Mr. P. Kertis and co-workers of Aberdeen Proving Ground for design and execution of low temperature firing tests and Mrs. T. Brassard of Long Beach Naval Shipyard for metallographic analysis.

TABLE OF CONTENTS

| | <u>Page</u> |
|--|-------------|
| DEDICATION | i |
| ACKNOWLEDGEMENTS | ii |
| INTRODUCTION | 1 |
| CASE I: MUZZLE CRACKING | 2 |
| Macroscopic Nature of Cracking | 2 |
| Microscopic Nature of Cracking | 7 |
| Residual Stress Measurement and Analysis | 9 |
| Stress Corrosion Tests | 14 |
| CASE II: OD SURFACE CRACKING | 17 |
| Nature of Cracking | 17 |
| Residual Stress | 20 |
| CASE STUDY IMPLICATIONS | 21 |
| Cause of Cracking | 21 |
| Effects on Service Life | 23 |
| Prevention of Stress Corrosion Cracking | 26 |
| REFERENCES | 29 |

TABLES

| | |
|--|----|
| I. SERVICE CONDITIONS AND ADDITIONAL TESTS FOR 105-MM TUBES WITH MUZZLE CRACKS | 5 |
| II. MECHANICAL PROPERTIES OF 105-MM TUBE MATERIAL | 11 |
| III. FREQUENCY AND POSITION OF RADIAL CRACKS IN SECTION OF 105-MM TUBE #251 FOLLOWING 90-MINUTE IMMERSION IN NBS STRESS CORROSION CRACKING TEST SOLUTION | 16 |
| IV. SERVICE CONDITIONS AND TEST RESULTS FOR 155-MM TUBES | 19 |

LIST OF ILLUSTRATIONS

| | |
|---|----|
| 1. Ultrasonic measurements of location and depth of muzzle cracks in 105-mm tube #156. | 3 |
| 2. Fracture surface of tube #156; 200-mm long segment of tube shown, including 102-mm long crack perforation on OD surface (1X). | 4 |
| 3. Polished and etched cross-section of a portion of tube #156 showing crack growth from ID to OD and locations of additional investigation (15X). | 7 |
| 4. Cracks and fracture surfaces for tube #156: | 8 |
| (a) Photomicrograph of location a in Figure 3 showing cracks from the land fillet (100X). | |
| (b,c,d) SEM fractographs at locations b, c, d in Figure 3 (400X, 100X, 1700X, respectively). | |
| 5. Intergranular crack growth for tube #190: | 10 |
| (a) SEM fractograph of primary crack at ID surface (350X) (similar to location b in Figure 3). | |
| (b) Photomicrograph of section intersecting primary fracture surface near ID surface (1000X). | |
| 6. Measured and analytical residual stress distributions for 105-mm tube #190. | 12 |
| 7. Measured and analytical residual stress for 105-mm tube #866. | 14 |
| 8. Macrophotograph of radial cracks in section of 105-mm tube #251 following 90-minute immersion in NBS stress corrosion cracking test solution (7X); ultraviolet illumination following magnetic particle NDT procedure. | 17 |
| 9. Prior laboratory fatigue crack initiation and growth from the thread sector fillet; also shown are typical locations a and b of apparent stress corrosion cracking in two 155-mm tubes. | 18 |
| 10. Ultraviolet light photograph of magnetic particle indications of stress corrosion cracking in 155-mm tube #193 in thread sector Fillet, see location a in Figure 9 (2X). | 20 |

INTRODUCTION

Stress corrosion cracking of A723 high strength steel forgings used for cannon is a significant concern, since the three conditions required for this type of fracture are sometimes present with cannon - a susceptible material, an aggressive chemical environment, a sustained tensile stress. Some consideration has been given to environmentally assisted fracture of cannon in prior work. In a case study of a cannon failure (ref 1), corrosion fatigue was identified as a likely contributing factor to growth of the crack which initiated a classically brittle, fragmentation-type failure of the cannon. Liquid metal embrittlement of A723 steel by lead was shown (refs 2,3) to cause the failure of several cannon during manufacture. Two comprehensive test series by Clark (refs 4,5) used a forged high strength steel very similar to A723 to address initiation and growth of stress corrosion cracks in hydrogen sulfide, a common by-product of cannon firing.

The purpose here is to describe two separate series of incidents of apparent stress corrosion cracking in cannon and to thereby learn more of the cause and prevention of this type of fracture in cannon and pressure vessels in general.

¹T. E. Davidson, J. F. Throop, and J. H. Underwood, "Failure of a 175 mm Cannon Tube and the Resolution of the Problem Using an Autofrettaged Design," Case Studies in Fracture Mechanics, (T. P. Rich and D. J. Cartwright, eds.), AMMRC MS 77-5, Army Materials and Mechanics Research Center, 1977, pp. 3.9.1-3.9.13.

²M. H. Kamdar, "Embrittlement of Gun Steel by Liquid Lead," ARRADCOM Report ARLCB-TR-77046, Benet Weapons Laboratory, Watervliet, NY, December 1977.

³M. H. Kamdar, "Embrittlement of 4340 Type Steel by Liquid Lead and Antimony and Lead-Antimony Solutions," Embrittlement by Liquid and Solid Metals, (M. H. Kamdar, ed.), AIME, 1983, pp. 149-159.

⁴W. G. Clark, Jr., "Applicability of the K_{ISCC} Concept to Very Small Defects," Cracks and Fracture, ASTM STP 601, ASTM, 1976, pp. 138-153.

⁵W. G. Clark, Jr., "Stress-Corrosion Crack Initiation in High-Strength Type 4340 Steel," Flow Growth and Fracture, ASTM STP 631, ASTM, 1977, pp. 121-138.

CASE I: MUZZLE CRACKING

Macroscopic Nature of Cracking

During the late 1970's muzzle cracking of the 105-mm inner diameter (ID) cannon was reported at Army proving grounds. Cracks were noted on the outer diameter (OD) surface of the cannon within about one meter of the muzzle end of the tube. Investigation of the cracking began with a thorough ultrasonic survey of the muzzle end of the first tube in which OD cracks were observed. An end-on pulse-echo ultrasonic method, developed for nondestructive investigation of cannon (ref 6), was used to map out the location and depth of cracks emanating from the ID surface, see Figure 1. Crack depths of 0.5 to 1.0 mm can be detected with the ultrasonic method. However, only depths of 1.5 mm and greater are indicated in Figure 1 to limit the amount of data shown. For tube #156 shown in Figure 1, the cracking occurred over a total included angle of about 90 degrees and in locations from about 60 to 380 mm from the muzzle end of the tube. The orientation of the cracks observed on the OD surface and those growing from the ID both seem to follow the helical pattern of the cannon rifling.

The same general pattern of extensive cracking from the ID and occasional cracks on the OD has been noted in a number of tubes. Table I lists 13 tubes in which muzzle cracking has been noted, along with service and test conditions which apply to these 13 tubes. Groups 1 and 4 are tubes in which cracks were observed with the unaided eye on the OD surface. Groups 2 and 3 are tubes in which cracks were located by ultrasonics with depths partway through from the ID

⁶D. P. Kendall, J. H. Underwood, and D. C. Winters, "Fracture Toughness Measurement and Ultrasonic Crack Measurement in Thick-Wall Cylinder Geometries," High Pressure Engineering, The Institution of Mechanical Engineers, London, 1977, pp. 255-263.

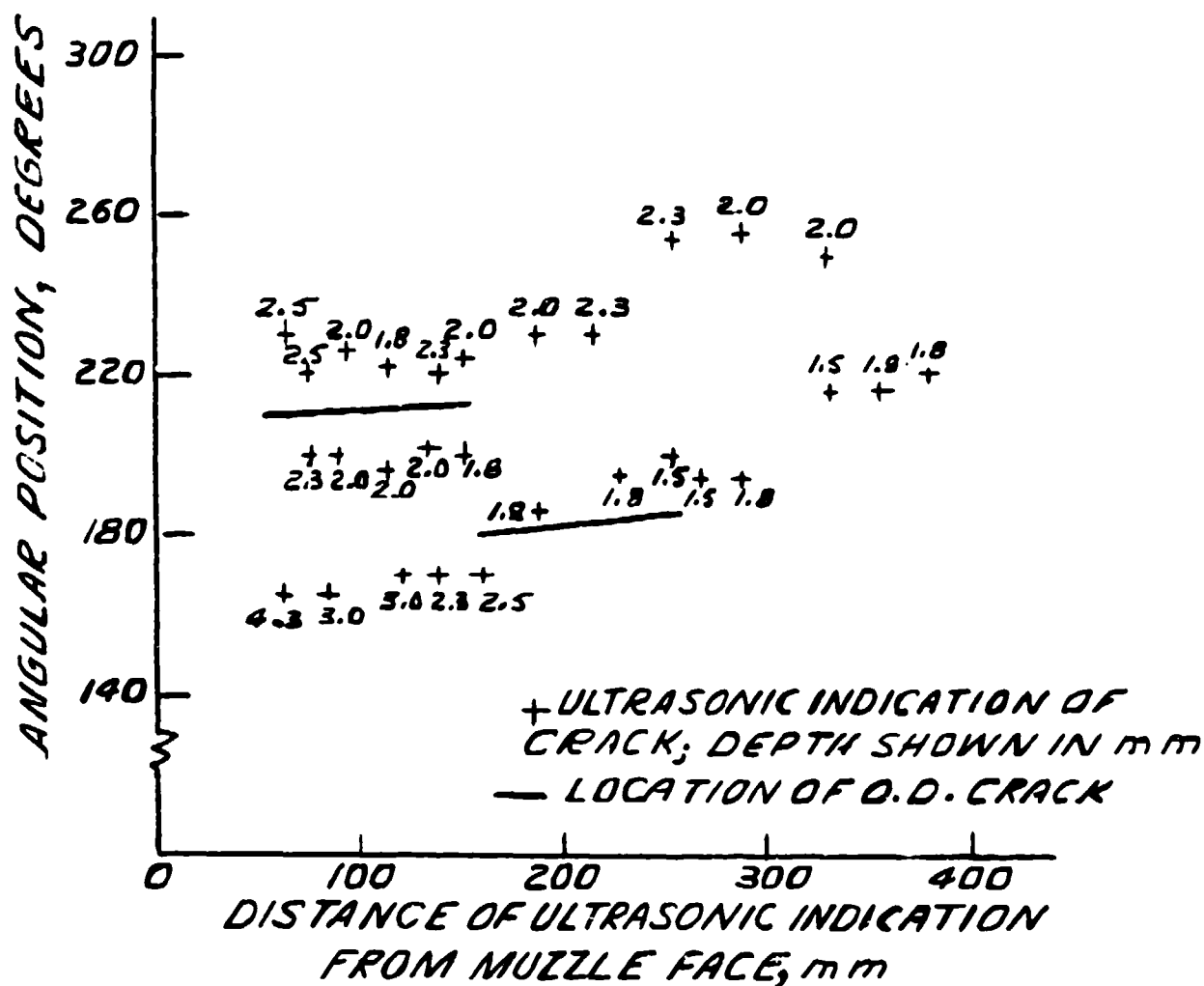
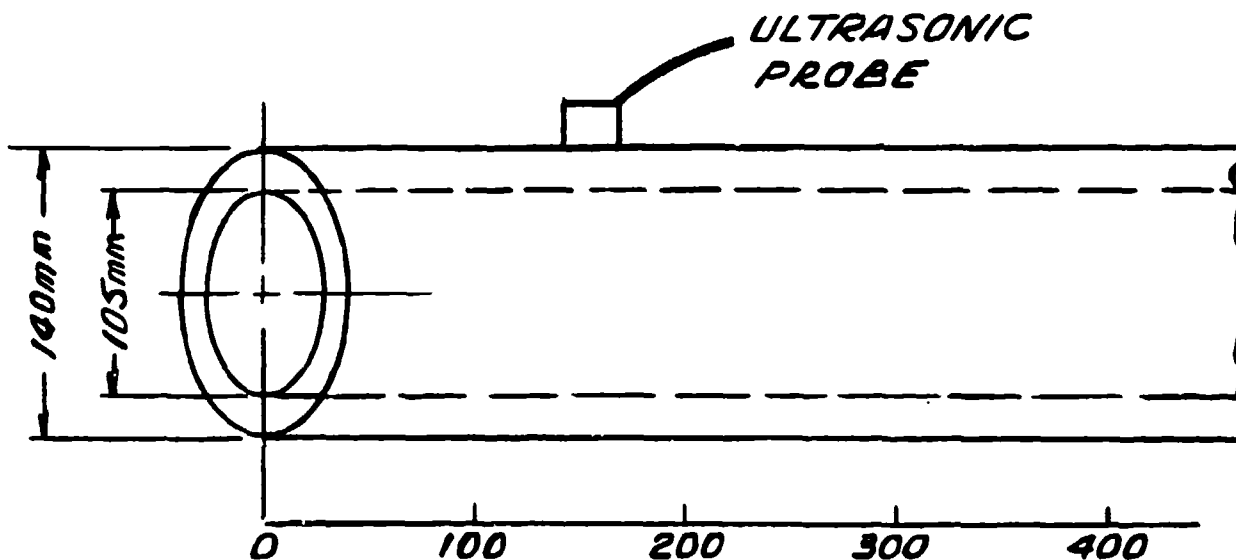


Figure 1. Ultrasonic measurements of location and depth of muzzle cracks in 105-mm tube #156.

to the OD. The firing cycles listed for each tube give some indication of the cumulative exposure to service firing conditions. The additional laboratory and firing tests which were performed with some of the tubes will be discussed in upcoming sections of this report.

The overall nature of the cracking, regarding macroscopic size and shape, was well revealed when the first tube which showed OD surface cracks was broken open, see Figure 2. This fracture surface was typical of those from tubes of Table I, in that three distinct regions can be seen. The first, a dark region near the ID surface, appears by its dark color to have existed for some time. An intermediate region made up of semielliptical-shaped, light areas, was the result of relatively recent fatigue cracking. The region near the OD surface was the result of the final, fast jump of the crack through to the OD surface. A 102-mm long portion of this final failure is believed to have occurred during one of the last firing cycles applied to this tube. The remaining final failure shown in Figure 2 occurred in our laboratory when the tube was broken open.



Figure 2. Fracture surface of tube #156; 200-mm long segment of tube shown, including 102-mm long crack perforation on OD surface (1X).

TABLE I. SERVICE CONDITIONS AND ADDITIONAL TESTS FOR 105-MM TUBES WITH MUZZLE CRACKS

| Tube # | Initial Conditions | | | | Following Additional Tests | | |
|-----------------|--------------------|-----------------------------------|-----------------------------------|------------------------------|----------------------------|--------------|-------------------------------------|
| | Firing Cycles | Crack Length on OO Surface 2c; mm | Crack Depth From ID Surface a; mm | Distance From Muzzle Face mm | Type of Test | Total Cycles | Final Crack Length on OO Surface mm |
| <u>Group 1:</u> | | | | | | | |
| 156 | 11,127 | 102 | thru | 200 | - | - | - |
| 664 | 14,504 | 152 | thru | 610 | - | - | - |
| 190 | 16,131 | 178 | thru | 230 | - | - | - |
| <u>Group 2:</u> | | | | | | | |
| 467 | 18,163 | 0 | 10 | 400 | <u>Laboratory:</u> | 18,615 | 25 |
| 227 | 14,688 | 0 | 8 | 470 | at +20°C | 16,651 | 30 |
| 372 | 16,234 | 0 | 7 | 580 | | 18,269 | 211 |
| 101 | 14,688 | 0 | 9 | 340 | | 15,630 | 15 |
| <u>Group 3:</u> | | | | | | | |
| 251 | 1,026 | 0 | <2 | - | <u>Laboratory:</u> | 23,228 | 132 |
| 866 | 869 | 0 | <2 | - | at +20°C | 24,355 | 15 |
| <u>Group 4:</u> | | | | | | | |
| 097 | 22,381 | 18 | thru | 260 | <u>Firing:</u> | 22,505 | 57 |
| 364 | 20,729 | 75 | thru | 330 | -26 to -54°C | 20,918 | 86 |
| 614 | 20,973 | 95 | thru | 440 | | 21,040 | 662 |
| 002 | 17,591 | 67 | thru | 390 | | 17,711 | 73 |

The most puzzling aspect of the fracture surface shown in Figure 2 was the orientation of the crack during its first region of growth, near the ID surface. The crack, soon after initiating at the ID surface, turned to a generally circumferential direction for a considerable distance, as opposed to the nearly universally observed radial direction crack growth in cannon tubes. This circumferential direction cracking, observed with 11 of the 13 tubes in Table I, cannot be easily explained. Crack growth is expected in the radial direction, in response to the circumferential direction tensile stresses in a pressurized cylinder. Cracking in the circumferential direction is not expected, because no significant tensile stresses are expected in the direction normal to this crack plane, that is, the radial direction. By definition, the radial direction tensile stress at the ID surface must be zero.

Additional evidence of the unexpected circumferential direction cracking is shown in Figure 3. Initiation of cracking can be seen at each of the rifling land fillets, such as location (a). The crack which eventually grows through to the OD surface starts at location (b), at the fillet of the unseen land to the left. Soon after this primary crack left the ID surface, it began to turn, so that when it reached location (c), its direction was almost directly circumferential. Cracks which have grown at least to the extent of location (c) are very easily located using the end-on ultrasonic method (ref 6), because a crack of this orientation presents a nearly planar surface approximately normal to the ultrasonic beam, and this results in a strong reflection. As the crack grew further, it eventually turned back toward a generally radial direction and

⁶D. P. Kendall, J. H. Underwood, and D. C. Winters, "Fracture Toughness Measurement and Ultrasonic Crack Measurement in Thick-Wall Cylinder Geometries," High Pressure Engineering, The Institution of Mechanical Engineers, London, 1977, pp. 255-263.

resumed growth toward the OD surface, location (d). Microstructural and fractographic details at these locations are given in the next section.

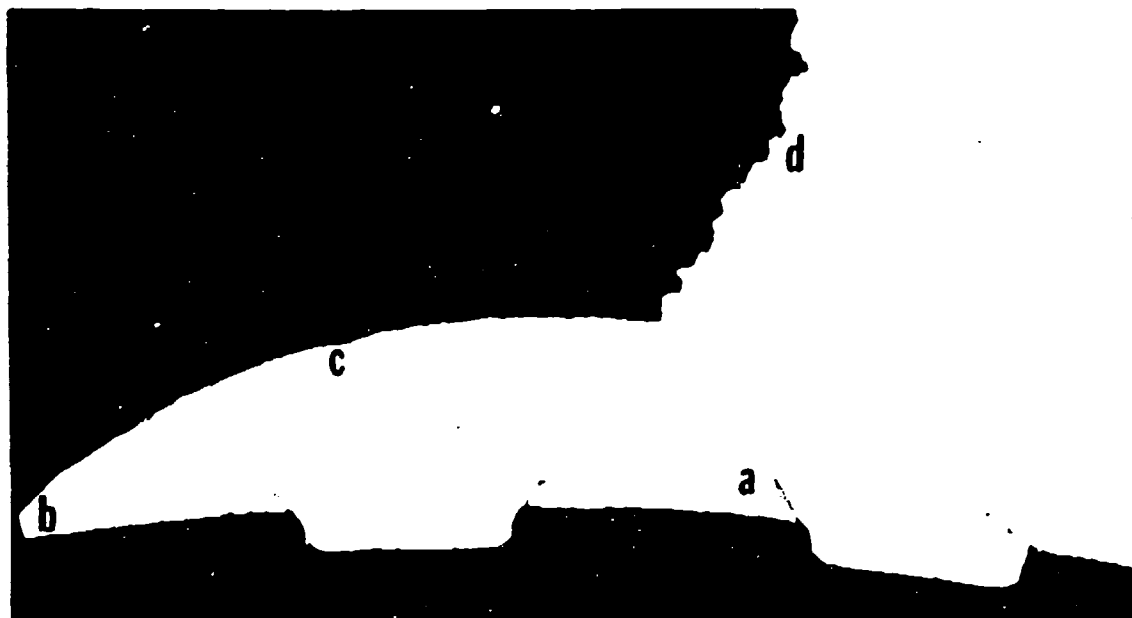


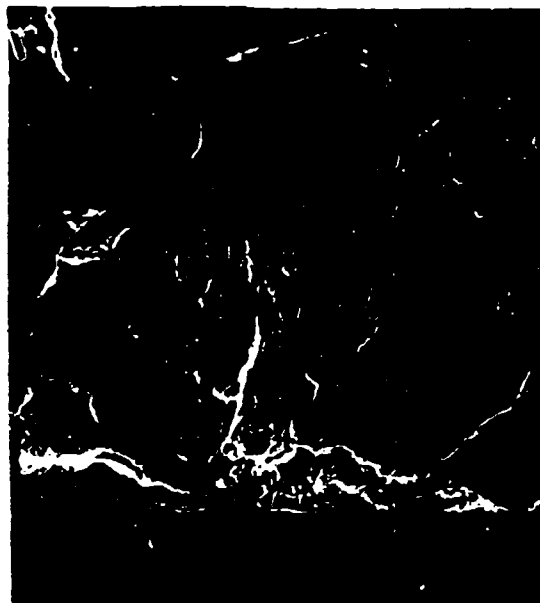
Figure 3. Polished and etched cross-section of a portion of tube #156 showing crack growth from ID to OD and locations of additional investigation (15X).

Microscopic Nature of Cracking

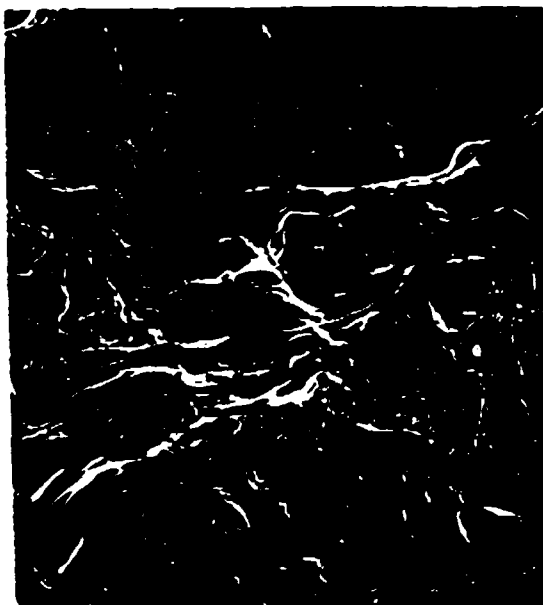
Figure 4 is a series of photomicrographs and fractographs at the locations shown in Figure 3. Figure 4a shows the multiply-branched nature of the cracks which occur at the land fillets, location (a). Figure 4b shows a relatively featureless fracture surface with some indication of secondary cracking at location (b) of the primary crack. These characteristics in Figures 4a and b - multiple branching, featurelessness, and secondary cracking - are all indications of stress corrosion cracking, as opposed to cracking due to mechanical loads, such as fatigue and fast fracture. Farther in the growth of the primary crack shown in Figure 3, evidence of both fatigue and fast fracture was observed. Figure 4c shows typical morphology of fatigue cracking, and Figure 4d shows the dimpled rupture of fast fracture.



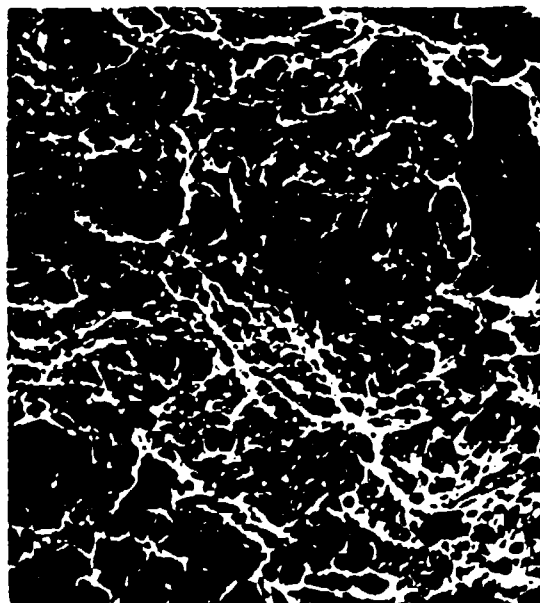
(a)



(b)



(c)



(d)

Figure 4. Cracks and fracture surfaces for tube #156:

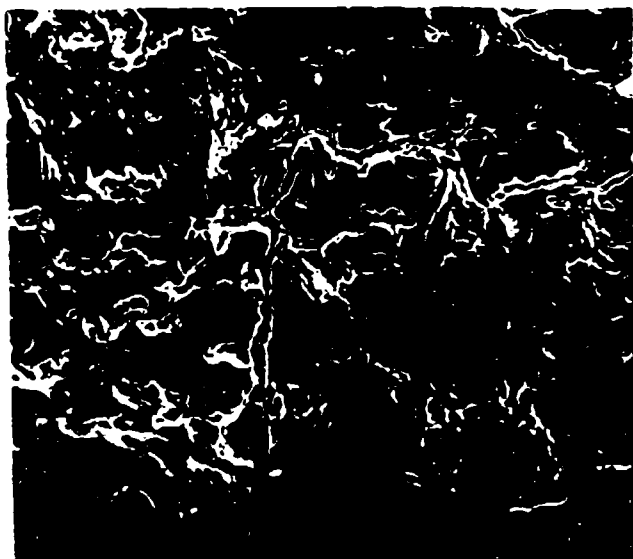
- (a) Photomicrograph of location a in Figure 3 showing cracks from the land fillet (100X).
- (b,c,d) SEM fractographs at locations b, c, d in Figure 3 (400X, 100X, 1700X, respectively).

Another strong indication of stress corrosion cracking is intergranular crack growth. Such crack growth was often observed near the ID surface. Metallographic investigation of tube #190 shows clear indications of intergranular cracking. In Figure 5a the fracture surface of the primary crack is relatively featureless, and the secondary cracking has an intergranular appearance. In Figure 5b the secondary cracking which intersects the primary crack surface is clearly intergranular along the prior austenitic grain boundaries.

Residual Stress Measurement and Analysis

Cannon tubes are often autofrettaged, as were the 105-mm tubes under consideration here. A hydraulic overpressure was applied, so that as usual with autofrettage, following the plastic deformation which executes the autofrettage, compressive residual stress remains near the ID surface and tensile residual stress remains near the OD surface. The pressure used for this tube was well in excess of the 100 percent overstrain pressure which produces plastic deformation throughout the relatively thin wall at the muzzle end of the tube. An external container was used to limit the plastic dilation of the tube.

The circumferential direction compressive residual stresses which should be present following autofrettage of this tube would be expected to absolutely prevent any type of stress corrosion cracking at or near the ID surface. However, because of the many indications of stress corrosion cracking shown in Figures 1 through 5, measurements and analysis were performed to determine the state of residual stress in the muzzle end of the tube. Figure 6 shows some of the results. First, the circumferential direction residual stress, σ_θ , can be



(a) SEM fractograph of primary crack at ID surface (350X) (similar to location b in Figure 3).



(b) Photomicrograph of section intersecting primary fracture surface near ID surface (1000X).

Figure 5. Intergranular crack growth for tube #190.

calculated from classical plasticity analysis (ref 7) for the 100 percent overstrain condition,

$$\sigma_{\theta}/\sigma_y = 1 + \ln(r/r_1) - \ln(r_2/r_1) \left[1 + \frac{r_1^2}{r_2^2 - r_1^2} \left(1 + \frac{r_2^2}{r^2} \right) \right] \quad (1)$$

where σ_y is yield strength and r , r_1 , r_2 are radius, inner radius, and outer radius, respectively. Values of r_1 and r_2 are from Figure 1, and σ_y is available from Table II. The material properties in Table II are from original tests of the tube forging and from recent tests of two tubes as part of this case study. Note that the recent tests show a significant increase in strength and a decrease in impact energy. These changes are not scatter, but rather the result of the plastic deformation associated with autofrettage.

TABLE II. MECHANICAL PROPERTIES OF 105-MM TUBE MATERIAL

| Tube # | Yield Strength | | Notched Impact Energy, -40°C | | Fracture Toughness Recent Tests MPa m ^{1/2} |
|--------|----------------|---------------------|------------------------------|-------------------|--|
| | Forging MPa | Recent Tests MPa | Forging J | Recent Tests J | |
| 664 | 1180, 1190 | 1270, 1290 | 30, 31 | 25, 27 | - |
| 190 | 1180, 1190 | 1300, 1330 | 29, 30 | 22, 23, 22, 24 | 109, 108, 107, 116 |

Three independent measurements of residual stress were performed on segments from the muzzle end of tube #190, see Figure 6. The strain gage tests used the simple concept often used to measure residual stress, of cutting away most of the material around a gage which was mounted on the component while it was still whole. The strains relieved from one gage each on the OD and ID surfaces of the tube were used to calculate the stresses at these points. The slitting test used a slice cut from the tube which was slit and measured to determine the angle of opening, γ , see Figure 6. Values of circumferential

⁷R. Hill, The Mathematical Theory of Plasticity, Oxford University Press, 1950.

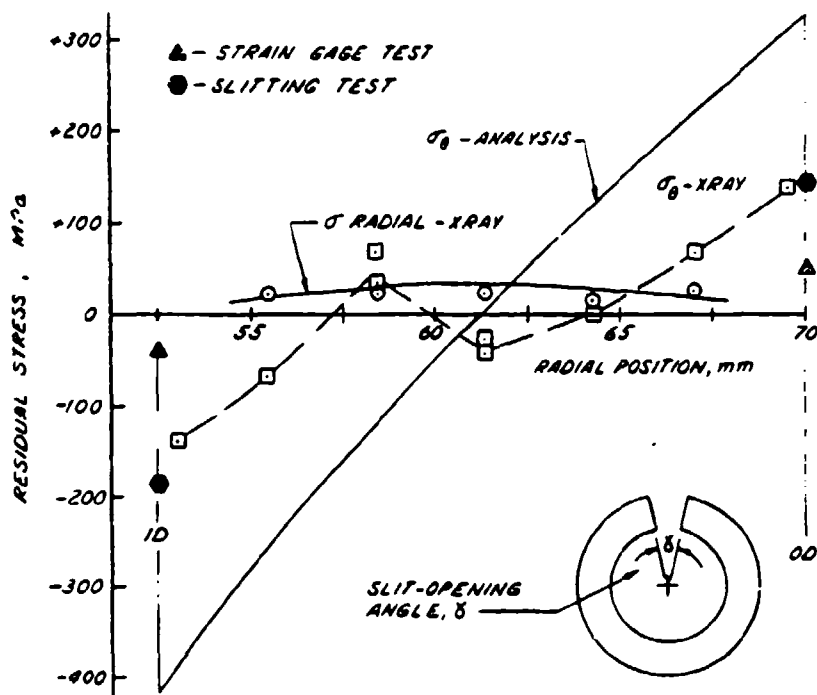


Figure 6. Measured and analytical residual stress distributions for 105-mm tube #190.

direction residual stress, σ_s , can be calculated using the measured angle of slit opening, γ_m , as follows,

$$\sigma_s = \sigma_\theta(\gamma_m/\gamma_t) \quad (2)$$

where γ_m is obtained from

$$\gamma_m = \tan^{-1}(\Delta/r_2) \quad (3)$$

in which Δ is the measured opening on the tube OD surface. The theoretical value of slit opening, γ_t , for a full overstrain condition is (ref 8):

$$\gamma_t = 4.62 \pi \sigma_y / E \quad (4)$$

⁸A. P. Parker, J. H. Underwood, J. F. Throop, and C. P. Andrasic, "Stress Intensity and Fatigue Crack Growth in a Pressurized, Autofrettaged Thick Cylinder," Fracture Mechanics: Fourteenth Symposium - Volume I: Theory and Analysis, ASTM STP 791, (J. C. Lewis and G. Sines, eds.), ASTM, 1983, pp. I-216-I-237.

in which E is elastic modulus, 207,000 MPa, and γ_t is given in radians. For the mean value of strength in Table II, $\gamma_t = 5.2$ degrees, whereas the measured opening angle for the tube was 2.3 degrees. Therefore, by this measure, the residual stress in tube #190 was less than half that predicted by analysis. The slitting test residual stress values shown in Figure 6, calculated from Eqs. (1) through (4), reflect this significant difference between measurement and analysis.

The third type of measurement of residual stress used for the results in Figure 6 is the well-known x-ray method (ref 9). It is clear that the three sets of measurements are not in close agreement. This is a reflection of the inherent difficulty in measuring residual stress, particularly in a failed component after many years of service. The important point is that the results from the three independent methods all lead to the same basic conclusion, that the measured residual stress in tube #190 is significantly below that expected from analysis. Lower than expected residual stresses can occur for some autofrettage conditions due to the Bauschinger effect (ref 8), which can significantly reduce the yield strength of the high strength steel used for cannon. However, a significant Bauschinger effect has not been observed for an r_2/r_1 as low as 1.33, the value for the tubes considered here.

X-ray residual stress measurements were made at eight locations on the OD surface of another tube, #866. The results, shown in Figure 7, are similar to those in Figure 6, that is, the x-ray measurements and the measurement from a

⁸A. P. Parker, J. H. Underwood, J. F. Throop, and C. P. Andrasic, "Stress Intensity and Fatigue Crack Growth in a Pressurized, Autofrettaged Thick Cylinder," Fracture Mechanics: Fourteenth Symposium - Volume I: Theory and Analysis, ASTM STP 791, (J. C. Lewis and G. Sines, eds.), ASTM, 1983, pp. I-216-I-237.

⁹B. D. Cullity, Elements of X-Ray Diffraction, Addison-Wesley, Reading, MA, 1956, pp. 431-453.

slitting test are considerably below that from analysis. In addition, the x-ray results indicate that whatever caused a reduction in residual stress in this tube did so in an approximately circularly-symmetric manner.

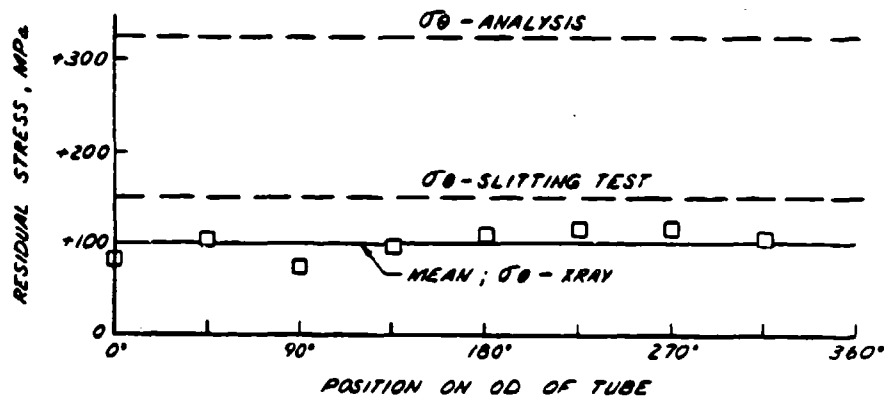


Figure 7. Measured and analytical residual stress for 105-mm tube #866.

Stress Corrosion Tests

The final type of testing performed in the muzzle cracking investigation was subjecting tube sections to a known stress corrosion cracking environment. If stress corrosion cracks were observed in a laboratory environment, this would be further evidence that stress corrosion cracking had occurred in the tubes in the service environment. These tests were planned primarily as confirmation of the presence of tensile residual stress, since the evidence was mixed in this regard.

Several disks, about 25-mm thick in the axial direction, were cut from tubes #372 and #251, surface ground, and visually and magnetic particle inspected for cracks, looking primarily at the ID surface in the land fillets. The disk locations were chosen as close as possible to the locations of the

cracks observed in service, but with care not to include any service cracks. The presence of pre-existing service cracks in the disks could have relieved any tensile residual stress which might have been present.

The disks were immersed for 90-minute intervals in an aqueous solution which has become a standard and quite severe environment for stress corrosion cracking testing of high strength steels (ref 10), the "sour" or "sulfide cracking" test solution. It is 3.5 percent NaCl solution plus 0.5 percent acetic acid, periodically saturated with H_2S . Two of the several disks tested showed cracking. Magnetic particle inspection of a disk from tube #372 showed cracks of 0.1 to 0.4-mm length, following one 90-minute immersion. A disk from tube #251 showed many cracks, 37 in total, of 0.1 to 0.8-mm length, following two 90-minute immersions, see Figure 8. Table III shows the frequency and location of occurrence. There is little chance that these cracks had been present before exposure to the test solution, because the same magnetic particle inspection was performed before and after exposure. Also, the nature of the cracking is quite different, as can be seen by comparing Figures 3 and 8. The difference in direction of the cracking shown in the two figures may be due to the presence of applied mechanical loading in service, Figure 3, and only residual stress loading in the laboratory, Figure 8. The important point is that the growth of the cracks upon exposure to the test solution could have occurred only in the presence of a sustained tensile stress, a residual stress in this case.

A discussion of test results from the muzzle cracking case study and their implications as to the cause and prevention of stress corrosion cracking will be given following presentation of the second case study.

¹⁰B. F. Brown, Stress Corrosion Cracking Control Measures, NBS Monograph 156, National Bureau of Standards, 1977, pp. 43-54.

TABLE III. FREQUENCY AND POSITION OF RADIAL CRACKS IN SECTION OF 105-MM TUBE #251 FOLLOWING 90-MINUTE IMMERSION IN NBS STRESS CORROSION CRACKING TEST SOLUTION

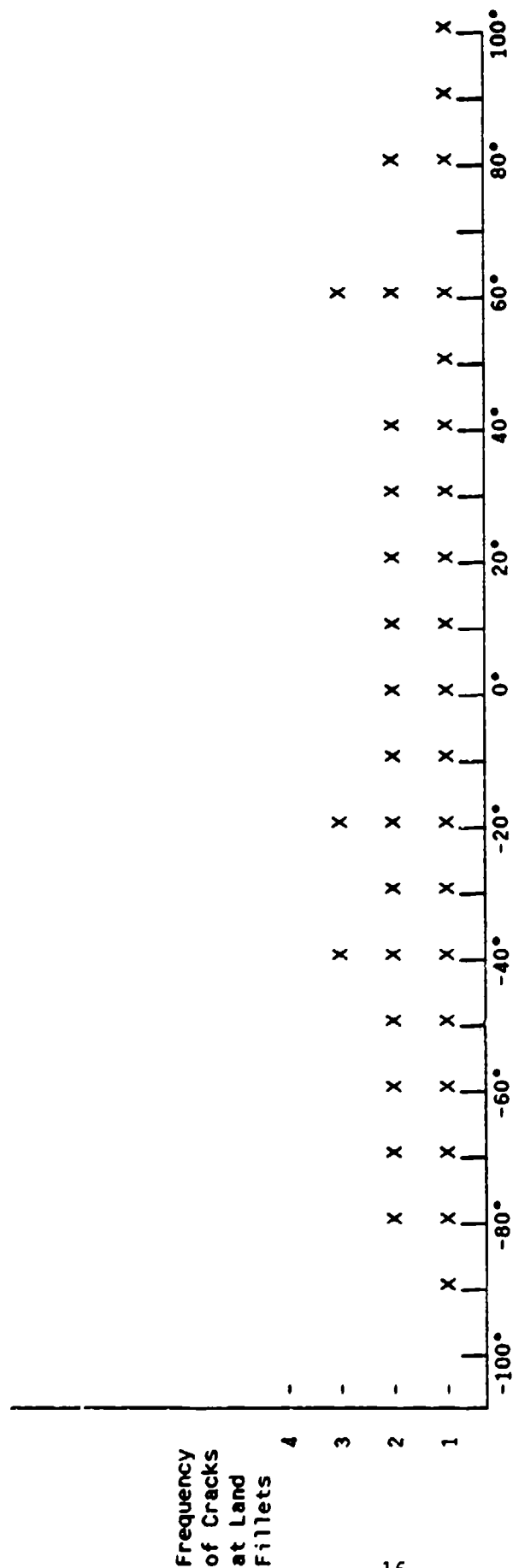




Figure 8. Macrophotograph of radial cracks in section of 105-mm tube #251 following 90-minute immersion in NBS stress corrosion cracking test solution (7X); ultraviolet illumination following magnetic particle NDT procedure.

CASE II: OD SURFACE CRACKING

Nature of Cracking

During 1984 and 1985, an unusual type of cracking of two 155-mm tubes was reported at an Army depot. Areas of cracking were observed on the OD surface of the breech end of the tubes. Figure 9 shows the general location of the cracking, marked a and b, and also a more common type of cracking which is often observed at the breech end of a cannon tube. The single crack seen in Figure 9 is due to prior, cyclic, mechanical loading in the laboratory, quite a different phenomenon from that considered here. However, the thread sector location is the same. A fatigue crack may initiate at the fillet of one of the thread sectors which are used to secure the end closure of the tube. The stress concentration factor of the raised thread sector is sometimes great enough to cause fatigue crack initiation at this fillet location. One of the two tubes under consideration showed the unusual cracking in the area of a thread sector fillet, and the cracking appeared to be of a different type than the single fatigue

crack shown in Figure 9. This suggests that, in addition to the relatively well-understood fatigue cracking, another type of cracking, possibly stress corrosion cracking, may affect the service life of these 155-mm tubes.

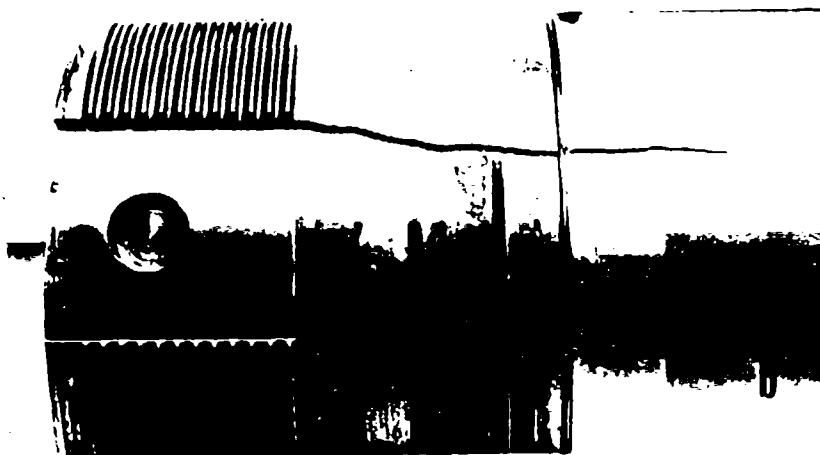


Figure 9. Prior laboratory fatigue crack initiation and growth from the thread sector fillet; also shown are typical locations a and b of apparent stress corrosion cracking in two 155-mm tubes.

Some details of the cracking are given in Table IV, along with the strength and notched impact energy properties of the tube material and of a recently tested group of ten tubes with no cracks. Note the angular position of the area of cracking in both tubes was the bottom-center. This suggests that a liquid contaminating substance which collected by gravity at the lowest point, may have been responsible. If the OD surface had been covered, this could have aided in holding an infiltrating contaminant in contact with the surface. Such was the case. The end closure effectively covered the OD surface in the case of tube #193 at 100 mm from the breech face, and a dust shield covered the tube in the case of #839 at 1200 mm from the breech face.

An ultraviolet light photograph of magnetic particle indications is shown in Figure 10 for the area of cracking for tube #193. The main features revealed in this photograph are the fluorescent magnetic particles at the locations of cracks at the tube surface. However, the ends of several threads

TABLE IV. SERVICE CONDITIONS AND TEST RESULTS FOR 155-MM TUBES

| Tube # | Maximum Crack Length mm | Angular Position; From Top-Center Degrees | Distance From Breech End mm | Yield Strength MPa | | Notched Impact Energy; -40°C J | |
|---------------------|----------------------------|---|-----------------------------------|-----------------------|--------------|--------------------------------------|--------------|
| | | | | Forging | Recent Tests | Forging | Recent Tests |
| 193 | 5 | 180 | 100 | 1120, 1120 | - | 24, 30 | - |
| 839 | 2 | 180 | 1200 | 1140, 1150 | - | 35, 39 | - |
| Mean of 10 tubes | - | - | - | 1168 | 1221 | 27.4 | 24.5 |

can be seen, giving some reference as to size and location of the cracks. It can be seen that the most severe cracking occurred near the thread sector fillet.

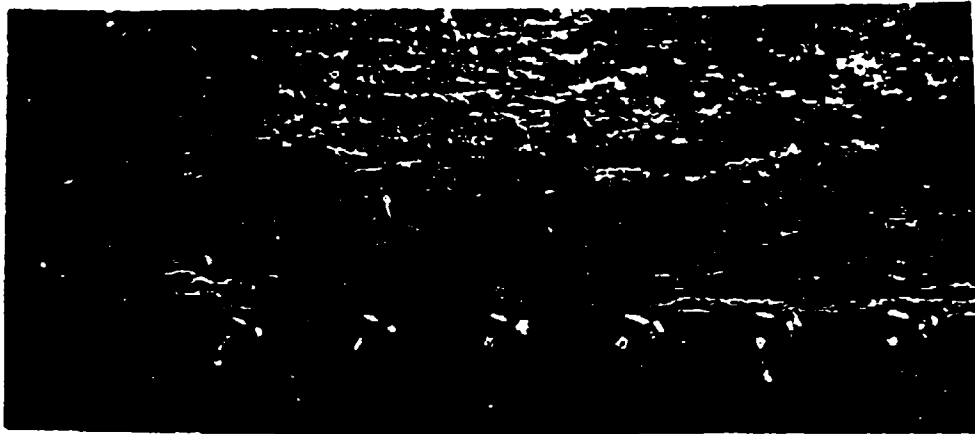


Figure 10. Ultraviolet light photograph of magnetic particle indications of stress corrosion cracking in 155-mm tube #193 in thread sector fillet, see location a in Figure 9 (2X).

Residual Stress

The 155-mm tubes were autofrettaged using the swage method, in which an oversized mandrel is forced through the tube to obtain a 100 percent overstrain condition. The value of residual stress at the OD surface can be calculated, based on classical plasticity analysis from Eq. (1), using the average value of yield strength from tubes #193 and #839, 1135 MPa, and nominal values of r_2 and r_1 , 140 and 80 mm, respectively. The circumferential direction, tensile residual stress obtained is:

$$\sigma_\theta = 518 \text{ MPa} \quad (5)$$

This calculated residual stress can be compared with a measured value based on slit openings, Δ , from the group of ten 155-mm tubes, which were autofrettaged in the same manner as the two under consideration here. The Δ values from ten tubes varied from 9.9 to 11.5 mm. Using the mean value, 10.8 mm, and Eqs. (2) through (4), gives

$$\sigma_s = 501 \text{ MPa} \quad (6)$$

The good agreement between calculated and measured residual stresses, Eqs. (5) and (6), clearly indicates that there was sufficient tensile residual stress present at the OD surface of the 155-mm tubes for stress corrosion cracking to occur. This is particularly true at the thread sector fillet where this nominal stress is concentrated. An important question in this case study is what aggressive environment was present. Unfortunately, this question cannot be answered with much certainty. Some possibilities will be discussed in the next section.

CASE STUDY IMPLICATIONS

Cause of Cracking

We believe that stress corrosion cracking controlled the initiation and early growth of the muzzle cracks in the 105-mm tubes and the full extent of cracking observed on the OD surfaces of the 155-mm tubes. Several of the classic indications and conditions for stress corrosion cracking were present, and the cracking was notably different from the mechanically driven crack growth often seen in cannon tubes.

In the case of the muzzle cracking, we believe that the entire early growth of the cracks, such as that shown in Figure 4a, was predominantly stress corrosion cracking. Of the three basic requirements for stress corrosion cracking - a sustained tensile stress, a susceptible material, an aggressive environment - the first and second relate directly to service conditions which were substantially altered from the norm for these tests. We believe that there was an unanticipated area of circumferential direction tensile residual stress within a few millimeters of the ID surface of the tube. The tensile residual stress may have been related somehow to the high-overpressure, hydraulic method used for the autofrettage of these tubes, but so much time has passed since the

tubes were made, this is little more than speculation. The unanticipated area of circumferential direction tensile residual stress also provides an explanation for the puzzling circumferential direction crack growth shown in Figure 3. The circumferential tensile stress caused the stress corrosion cracking predominantly in the radial direction, normal to the stress direction, as expected. However, once the crack had grown through the area of tension, it faced a compressive stress, was forced to turn to the circumferential direction, and continued its growth in response to fatigue loads. The metallographic evidence in Figures 4b and 4c supports this line of reasoning.

The high-overpressure method used in autofrettage is quite certain to have caused the increase in the yield strength of the tube material, see Table II, and a related increase in susceptibility to stress corrosion cracking. The increase in the mean value of yield stress was from 1185 to 1298 MPa, significantly more than could be accounted for by material or test variability. It should also be noted that 1250 MPa is a strength level above which resistance to stress corrosion cracking drops particularly quickly (ref 10).

In the case of the OD surface cracking, it is the aggressive environment requirement for stress corrosion cracking which relates to the cause of the cracking. Measurements of sustained tensile residual stress agree well with the expected values, Eqs. (5) and (6), and the tube material does not appear to be highly susceptible, see Table IV. This leaves environment as the suspected abnormal service condition. The most likely aggressive environment would be a cleaning agent which was in aqueous solution or became an aqueous solution with added rain water. The solution became trapped between the OD surface of

¹⁰B. F. Brown, Stress Corrosion Cracking Control Measures, NBS Monograph 156, National Bureau of Standards, 1977, pp. 43-54.

the tube and its covering structure for a long enough period of time for stress corrosion cracking to occur.

Effects on Service Life

The effect of the stress corrosion cracking on the service behavior of the tubes can be determined in the case of the muzzle cracking by considering the test results in Table I, and in the case of the OD surface cracking by performing life calculations.

Referring to Table I, the group 3 tubes, which experienced relatively few firing cycles and relatively small initial cracks, produced total fatigue lives only marginally above the mean life of all tubes. The mean life of the 13 tubes, to the point of crack breakthrough to the OD surface, was 18,475 total cycles, 3778 cycles standard deviation. The group 3 tubes, in which cracks grew mainly by mechanical loading in the laboratory, had a mean life of 23,792 cycles, only 29 percent above the mean life of all tubes, most of which were significantly affected by stress corrosion cracking. Based on this comparison, stress corrosion cracking resulted in a relatively small decrease in fatigue life. A larger effect of environment might have been observed if the affected tubes had been compared to tubes which were totally unaffected by environment, but this was not possible.

The effect of the muzzle cracking on the final fast failure of the tubes can be determined from the results of the additional tests which were performed on the group 4 tubes, Table I. Low temperature firing tests were performed with these four tubes to determine the type of additional crack growth which would occur from the through-wall crack already present in the tube. From 67 to 189 firing cycles were applied to the group 4 tubes. The result in three of these tubes was a small amount of crack extension, from 6 to 39 mm. In the other

tube, #614, which had the longest initial through-wall crack length, the crack ran to the muzzle end of the tube during the 67th, and last, firing cycle. Since the tube had withstood 66 loading cycles at a nominal temperature of -40°C with a 95-mm long through-wall crack, this was leak-before-break behavior under very severe service conditions. It is no cause for alarm. It is, however, of interest to compare the K applied to tube #614 with the fracture toughness, K_{IC} of the tube material from Table II. The classic expression for a center-cracked plate can be used for applied K ,

$$K = \bar{\sigma}(\pi c)^{1/2} \quad (7)$$

where an average value of tensile stress, $\bar{\sigma}$ can be calculated from the thin, pressurized cylinder expression

$$\bar{\sigma} = \frac{pr_1}{r_2 - r_1} \quad (8)$$

This gives an expression for applied K

$$K = \frac{pr_1}{r_2 - r_1} (\pi \bar{c})^{1/2} \quad (9)$$

where p is internal pressure and \bar{c} is the average half-crack length in the axial direction. Using a nominal $p = 100 \text{ MPa}$, r_2 and r_1 from Figure 1, and $2c = 3/2$ (95 mm) to account for a longer crack near the ID surface than the 95-mm length on the OD, gives

$$K_{\text{applied}} (-40^{\circ}\text{C}) = 71 \text{ MPa m}^{1/2} \quad (10)$$

$$K_{IC} (+20^{\circ}\text{C}) = 110 \text{ MPa m}^{1/2}$$

The difference between K applied and K_{IC} may be due to the difference in temperature or to the approximations used in the analysis. The important point is that the final fast failure of the tube with a through-wall muzzle crack occurred when K applied was approximately equal to K_{IC} .

In the case of the OD surface cracking, calculations can show that the effect of environment is quite significant. In prior work (ref 11), a general expression was developed for calculating fatigue life of a pressure vessel, which can be used here to compare lives with and without the presence of stress corrosion cracking:

$$N_f = \frac{2[a_i^{-1/2} - a_f^{-1/2}]}{6.52 \times 10^{-12} [f p \pi^{1/2}]^3} \quad (11)$$

In Eq. (11), N_f is the fatigue life for growth of a crack from an initial depth, a_i , to a final depth, a_f ; the constant 6.52×10^{-12} is from the fatigue crack propagation rate equation (ref 11); $f = K/p(\pi a)^{1/2}$ is a dimensionless stress intensity factor, K parameter. Note that the constant in Eq. (11) is appropriate for a in meters and p in MPa. An expression for f can be obtained by combining the well-known relation for the circumferential direction stress on the OD surface of a tube,

$$\sigma = 2p/[(r_2/r_1)^2 - 1] \quad (12)$$

with the expression for K for a shallow semielliptical edge notch (ref 12):

$$K = f_s \sigma (\pi a)^{1/2} \quad (13)$$

where f_s varies from 0.73 for semicircular crack to 1.12 for a straight-fronted crack (ref 12).

Combining Eqs. (11), (12), and (13) gives a fatigue life expression which applies strictly for shallow cracks only, but since shallow cracks so dominate fatigue life, the expression is generally useful for describing growth of

¹¹J. H. Underwood and J. F. Throop, "Surface Crack K-Estimates and Fatigue Life Calculations in Cannon Tubes," Part-Through Crack Fatigue Life Prediction, ASTM STP 687, (J. B. Chang, ed.), ASTM, 1979, pp. 195-210.

¹²J. C. Newman, Jr. and I. S. Raju, "An Empirical Stress-Intensity Factor Equation for the Surface Crack," Engineering Fracture Mechanics, Vol. 15, No. 1-2, 1981, pp. 185-192.

semielliptical surface cracks on the OD surface of a pressurized cylinder.

$$N_f = \frac{[a_i^{-1/2} - a_f^{-1/2}]}{1.45 \times 10^{-10} \left[\frac{f_s p}{(r_2/r_1)^2 - 1} \right]^2} \quad (14)$$

Lives can be calculated from Eq. (14) using $a_i = 0.03$ mm, which is typical of the expected inclusion size of A723 steel, and $a_f = 2.5$ mm, the crack depth corresponding to a 5-mm long semicircular surface crack, see Table IV. The other nominal values used in the calculation are $a_f = 60$ mm, $f_s = 0.73$, $p = 300$ MPa, $r_2 = 140$ mm, $r_1 = 80$ mm. The results are:

$$\begin{aligned} \text{for natural inclusion:} \quad N_f &= 3.45 \times 10^6 \text{ cycles} \\ \text{for stress corrosion cracks:} \quad N_f &= 0.31 \times 10^6 \text{ cycles} \end{aligned} \quad (15)$$

This shows that even with the nonconservative assumption that no further stress corrosion cracking would occur, the effect on the fatigue life is a reduction by more than a factor of ten.

Prevention of Stress Corrosion Cracking

It is seldom possible to eliminate contact with the aggressive environment and thereby absolutely prevent stress corrosion cracking. In the muzzle cracking case, it could not be done since the environment is an integral part of cannon firing. In the OD surface cracking case, steps can and should be taken to minimize contact with potentially aggressive substances, such as aqueous salt solutions and acid solutions, particularly in the areas of the tube with covering structures which can entrap contaminants and allow them to accomplish their dirty work.

The susceptibility of the material can be controlled. The words of B. F. Brown (ref 10) describe it well, "A primary measure to avoid SCC should be the

¹⁰B. F. Brown, Stress Corrosion Cracking Control Measures, NBS Monograph 156, National Bureau of Standards, 1977, pp. 43-54.

selection of a steel with good SCC properties, in particular selecting one with no higher strength than is needed." The high strength of the material in the muzzle cracking case is believed to be a major contributing cause of the cracking. This same basic lesson was learned many years ago (ref 1) in the 175-mm tube failure and subsequent redesign, which centered on a reduction in the maximum allowed material yield strength from 1310 MPa to 1100 MPa. This approach is still valid today.

It is also possible to control the nature of the residual stresses resulting from autofrettage, in order to help prevent stress corrosion cracking. Autofrettage with partial overstrain, that is with plastic deformation proceeding just partway through the wall thickness, has several advantages. First, in comparison to a full overstrain, a partial overstrain reduces the tensile residual stresses near the OD surface of the tube in greater proportion than the reduction of the compressive residual stresses near the ID surface (ref 11). Thus, the likelihood of stress corrosion cracking near the OD surface is reduced, with no increased likelihood of stress corrosion cracking anywhere in the tube and only a slightly increased likelihood of mechanically controlled cracking near the ID surface. A second advantage of partial overstrain is that the increase in yield strength of the tube material is less than that associated with full overstrain. As already discussed, lower strength material is less

¹T. E. Davidson, J. F. Throop, and J. H. Underwood, "Failure of a 175 mm Cannon Tube and the Resolution of the Problem Using an Autofrettaged Design," Case Studies in Fracture Mechanics, (T. P. Rich and D. J. Cartwright, eds.), AMMRC MS 77-5, Army Materials and Mechanics Research Center, 1977, pp. 3.9.1-3.9.13.

¹¹J. H. Underwood and J. F. Throop, "Surface Crack K-Estimates and Fatigue Life Calculations in Cannon Tubes," Part-Through Crack Fatigue Life Prediction, ASTM STP 687, (J. B. Chang, ed.), ASTM, 1979, pp. 195-210.

susceptible to cracking. Another advantage of partial overstrain, although not easily demonstrated, is nonetheless important. Partial overstrain is believed to be much less affected by nonideal plastic deformation (ref 8). Thus, the overstrain process is better controlled, and the residual stresses resulting from the process are more certainly known. These are important advantages in dealing with stress corrosion cracking.

⁸A. P. Parker, J. H. Underwood, J. F. Throop, and C. P. Andrasic, "Stress Intensity and Fatigue Crack Growth in a Pressurized, Autofrettaged Thick Cylinder," Fracture Mechanics: Fourteenth Symposium - Volume I: Theory and Analysis, ASTM STP 791, (J. C. Lewis and G. Sines, eds.), ASTM, 1983, pp. I-216-I-237.

REFERENCES

1. T. E. Davidson, J. F. Throop, and J. H. Underwood, "Failure of a 175 mm Cannon Tube and the Resolution of the Problem Using an Autofrettaged Design," Case Studies in Fracture Mechanics, (T. P. Rich and D. J. Cartwright, eds.), AMMRC MS 77-5, Army Materials and Mechanics Research Center, 1977, pp. 3.9.1-3.9.13.
2. M. H. Kamdar, "Embrittlement of Gun Steel by Liquid Lead," ARRADCOM Report ARLCB-TR-77046, Benet Weapons Laboratory, Watervliet, NY, December 1977.
3. M. H. Kamdar, "Embrittlement of 4340 Type Steel by Liquid Lead and Antimony and Lead-Antimony Solutions," Embrittlement by Liquid and Solid Metals, (M. H. Kamdar, ed.), AIME, 1983, pp. 149-159.
4. W. G. Clark, Jr., "Applicability of the K_{Isc} Concept to Very Small Defects," Cracks and Fracture, ASTM STP 601, ASTM, 1976, pp. 138-153.
5. W. G. Clark, Jr., "Stress-Corrosion Crack Initiation in High-Strength Type 4340 Steel," Flow Growth and Fracture, ASTM STP 631, ASTM, 1977, pp. 121-138.
6. D. P. Kendall, J. H. Underwood, and D. C. Winters, "Fracture Toughness Measurement and Ultrasonic Crack Measurement in Thick-Wall Cylinder Geometries," High Pressure Engineering, The Institution of Mechanical Engineers, London, 1977, pp. 255-263.
7. R. Hill, The Mathematical Theory of Plasticity, Oxford University Press, 1950.
8. A. P. Parker, J. H. Underwood, J. F. Throop, and C. P. Andrasic, "Stress Intensity and Fatigue Crack Growth in a Pressurized, Autofrettaged Thick Cylinder," Fracture Mechanics: Fourteenth Symposium - Volume I: Theory and Analysis, ASTM STP 791, (J. C. Lewis and G. Sines, eds.), ASTM, 1983, pp. I-216-I-237.
9. B. D. Cullity, Elements of X-Ray Diffraction, Addison-Wesley, Reading, MA, 1956, pp. 431-453.
10. B. F. Brown, Stress Corrosion Cracking Control Measures, NBS Monograph 156, National Bureau of Standards, 1977, pp. 43-54.
11. J. H. Underwood and J. F. Throop, "Surface Crack K -Estimates and Fatigue Life Calculations in Cannon Tubes," Part-Through Crack Fatigue Life Prediction, ASTM STP 687, (J. B. Chang, ed.), ASTM, 1979, pp. 195-210.
12. J. C. Newman, Jr. and I. S. Raju, "An Empirical Stress-Intensity Factor Equation for the Surface Crack," Engineering Fracture Mechanics, Vol. 15, No. 1-2, 1981, pp. 185-192.

TECHNICAL REPORT INTERNAL DISTRIBUTION LIST

| | NO. OF COPIES |
|---|------------------|
| CHIEF, DEVELOPMENT ENGINEERING BRANCH | |
| ATTN: SMCAR-CCB-D | 1 |
| -DA | 1 |
| -DC | 1 |
| -DM | 1 |
| -DP | 1 |
| -DR | 1 |
| -DS (SYSTEMS) | 1 |
| CHIEF, ENGINEERING SUPPORT BRANCH | |
| ATTN: SMCAR-CCB-S | 1 |
| -SE | 1 |
| CHIEF, RESEARCH BRANCH | |
| ATTN: SMCAR-CCB-R | 2 |
| -R (ELLEN FOGARTY) | 1 |
| -RA | 1 |
| -RM | 1 |
| -RP | 1 |
| -RT | 1 |
| TECHNICAL LIBRARY | 5 |
| ATTN: SMCAR-CCB-TL | |
| TECHNICAL PUBLICATIONS & EDITING UNIT | 2 |
| ATTN: SMCAR-CCB-TL | |
| DIRECTOR, OPERATIONS DIRECTORATE | 1 |
| ATTN: SMCWV-OD | |
| DIRECTOR, PROCUREMENT DIRECTORATE | 1 |
| ATTN: SMCWV-PP | |
| DIRECTOR, PRODUCT ASSURANCE DIRECTORATE | 1 |
| ATTN: SMCWV-QA | |

NOTE: PLEASE NOTIFY DIRECTOR, BENET LABORATORIES, ATTN: SMCAR-CCB-TL, OF ANY ADDRESS CHANGES.

TECHNICAL REPORT EXTERNAL DISTRIBUTION LIST

| | <u>NO. OF COPIES</u> | | <u>NO. OF COPIES</u> |
|--|--------------------------|--|--------------------------|
| ASST SEC OF THE ARMY RESEARCH AND DEVELOPMENT ATTN: DEPT FOR SCI AND TECH THE PENTAGON WASHINGTON, D.C. 20310-0103 | 1 | COMMANDER ROCK ISLAND ARSENAL ATTN: SMCRI-ENM ROCK ISLAND, IL 61299-5000 | 1 |
| ADMINISTRATOR DEFENSE TECHNICAL INFO CENTER ATTN: DTIC-FDAC CAMERON STATION ALEXANDRIA, VA 22304-6145 | 12 | DIRECTOR US ARMY INDUSTRIAL BASE ENGR ACTV ATTN: AMXIB-P ROCK ISLAND, IL 61299-7260 | 1 |
| COMMANDER US ARMY ARDEC ATTN: SMCAR-AEE | 1 | COMMANDER US ARMY TANK-AUTMV R&D COMMAND ATTN: AMSTA-DOL (TECH LIB) WARREN, MI 48397-5000 | 1 |
| SMCAR-AES, BLDG. 321 | 1 | COMMANDER US MILITARY ACADEMY | 1 |
| SMCAR-AET-O, BLDG. 351N | 1 | ATTN: DEPARTMENT OF MECHANICS | |
| SMCAR-CC | 1 | WEST POINT, NY 10996-1792 | |
| SMCAR-CCP-A | 1 | US ARMY MISSILE COMMAND | |
| SMCAR-FSA | 1 | REDSTONE SCIENTIFIC INFO CTR | 2 |
| SMCAR-FSM-E | 1 | ATTN: DOCUMENTS SECT, BLDG. 4484 | |
| SMCAR-FSS-D, BLDG. 94 | 1 | REDSTONE ARSENAL, AL 35898-5241 | |
| SMCAR-MSI (STINFO) | 2 | | |
| PICATINNY ARSENAL, NJ 07806-5000 | | | |
| DIRECTOR US ARMY BALLISTIC RESEARCH LABORATORY ATTN: SLCBR-DD-T, BLDG. 305 | 1 | COMMANDER US ARMY FGN SCIENCE AND TECH CTR ATTN: DRXST-SD | 1 |
| ABERDEEN PROVING GROUND, MD 21005-5066 | | 220 7TH STREET, N.E. CHARLOTTESVILLE, VA 22901 | |
| DIRECTOR US ARMY MATERIEL SYSTEMS ANALYSIS ACTV ATTN: AMXSY-MP | 1 | COMMANDER US ARMY LABCOM | |
| ABERDEEN PROVING GROUND, MD 21005-5071 | | MATERIALS TECHNOLOGY LAB ATTN: SLCMT-IML (TECH LIB) | 2 |
| COMMANDER HQ, AMCCOM ATTN: AMSMC-IMP-L | 1 | WATERTOWN, MA 02172-0001 | |
| ROCK ISLAND, IL 61299-6000 | | | |

NOTE: PLEASE NOTIFY COMMANDER, ARMAMENT RESEARCH, DEVELOPMENT, AND ENGINEERING CENTER, US ARMY AMCCOM, ATTN: BENET LABORATORIES, SMCAR-CCB-TL, WATERVLIT, NY 12189-4050, OF ANY ADDRESS CHANGES.

TECHNICAL REPORT EXTERNAL DISTRIBUTION LIST (CONT'D)

| | <u>NO. OF COPIES</u> | | <u>NO. OF COPIES</u> |
|--|--------------------------|--|--------------------------|
| COMMANDER US ARMY LABCOM, ISA ATTN: SLCIS-IM-TL 2800 POWDER MILL ROAD ADELPHI, MD 20783-1145 | 1 | COMMANDER AIR FORCE ARMAMENT LABORATORY ATTN: AFATL/MN EGLIN AFB, FL 32543-5434 | 1 |
| COMMANDER US ARMY RESEARCH OFFICE ATTN: CHIEF, IPO P.O. BOX 12211 RESEARCH TRIANGLE PARK, NC 27709-2211 | 1 | COMMANDER AIR FORCE ARMAMENT LABORATORY ATTN: AFATL/MNF EGLIN AFB, FL 32542-5000 | 1 |
| DIRECTOR US NAVAL RESEARCH LAB ATTN: MATERIALS SCI & TECH DIVISION CODE 26-27 (DOC LIB) WASHINGTON, D.C. 20375 | 1 1 | METALS AND CERAMICS INFO CTR BATTELLE COLUMBUS DIVISION 505 KING AVENUE COLUMBUS, OH 43201-2693 | 1 |

NOTE: PLEASE NOTIFY COMMANDER, ARMAMENT RESEARCH, DEVELOPMENT, AND ENGINEERING CENTER, US ARMY AMCCOM, ATTN: BENET LABORATORIES, SMCAR-CCB-TL, WATERVLIET, NY 12189-4050, OF ANY ADDRESS CHANGES.